
Information matrices and generalization

Valentin Thomas*
Mila, Université de Montréal

Fabian Pedregosa
Google Brain

Bart van Merriënboer
Google Brain

Pierre-Antoine Mangazol
Google Brain

Yoshua Bengio
Mila, Université de Montréal
CIFAR Senior Fellow

Nicolas Le Roux
Google Brain
Mila, Université de Montréal

Abstract

This work revisits the use of *information criteria* to characterize the generalization of deep learning models. In particular, we empirically demonstrate the effectiveness of the Takeuchi information criterion (TIC), an extension of the Akaike information criterion (AIC) for misspecified models, in estimating the generalization gap, shedding light on why quantities such as the number of parameters cannot quantify generalization. The TIC depends on both the Hessian of the loss \mathbf{H} and the covariance of the gradients \mathbf{C} . By exploring the similarities and differences between these two matrices as well as the Fisher information matrix \mathbf{F} , we explore the interplay between noise and curvature in deep models. We also address the question of whether \mathbf{C} is a reasonable approximation to \mathbf{F} , as is commonly assumed.

1 Introduction

Deep networks generalize despite having far more parameters than the number of samples, a behaviour that is not captured by classic statistical measures of capacity such as the number of parameters, the L_2 norm of the parameters, or the VC dimension (Zhang et al., 2016). Recently, measures have been proposed that correlate better with the generalization abilities of these networks (Keskar et al., 2017; Neyshabur et al., 2017; Liang et al., 2017; Novak et al., 2018; Rangamani et al., 2019).

Rather than proposing a new metric, we empirically show how the Takeuchi information criterion (TIC: Takeuchi, 1976), an extension of the Akaike information criterion (AIC: Akaike, 1974), does not suffer from the limitations of the latter and can be applied to deep networks. In the case of linear models, AIC corresponds to counting the number of parameters. Under the assumption that the model is *well specified*¹, this can be seen as an estimator of the generalization gap. While this criterion is known to fail in the general case (see, e.g., Boué, 2019), the TIC extends to larger networks while matching the AIC on well-specified models. Worthy of note is that the TIC makes use of both the Hessian of the loss with respect to the parameters, \mathbf{H} , and the uncentered covariance of the gradients, \mathbf{C} . While the former represents the curvature of the loss, i.e., the sensitivity of the gradient to a change in parameter space, the latter represents the sensitivity of the gradient to a change in inputs. As the generalization gap is a direct consequence of the discrepancy between training and test sets, the influence of \mathbf{C} is natural. Thus, our result further reinforces the idea that the Hessian cannot by itself be used to estimate the generalization gap, an observation already made by Dinh et al. (2017), among others.

Since \mathbf{C} is sometimes referred to as the “empirical Fisher” matrix and assumed to be an approximation of the Fisher information matrix \mathbf{F} , we also explore the semantic and numerical relationship between

*Correspondence to: vltm.thomas@gmail.com

¹i.e., the data distribution is an element of the function class.

\mathbf{H} , \mathbf{F} and \mathbf{C} . After providing a counterexample where \mathbf{C} and \mathbf{H} can be arbitrarily different from each other, we observe that, in practice, they tend to be similar up to a scalar factor. This allows us to approximate the TIC with a much less computationally expensive metric.

This work makes the following contributions:

1. Through large-scale experiments, we empirically show that the TIC captures the generalization gap;
2. We theoretically and numerically explore the differences between \mathbf{H} , the Hessian, \mathbf{C} , the covariance of the gradients, and \mathbf{F} , the Fisher information matrix;
3. We use these numerical differences to propose two efficient approximations to the TIC.

2 Related work

Hastie et al. (2009) offer a review of classical methods for assessing the generalization performance of various models. Aside from methods reusing samples, such as cross-validation (Stone, 1974) and bootstrap (Efron, 1992), one of the simplest measures is the Akaike information criterion (AIC: Akaike, 1974). For well-specified linear models, the AIC is proportional to the number of parameters in the model divided by the number of samples in the training set. Under these assumptions, the AIC is asymptotically equivalent to *leave-one-out cross-validation* (Hastie et al., 2009) for a much lower computational cost.

An alternative to the AIC is the Bayesian information criterion (BIC: Schwarz et al., 1978) which favours simple models more heavily but is asymptotically consistent while the AIC is not. Less popular is the Takeuchi information criterion (TIC: Takeuchi, 1976) which is equal to $\text{Tr}(\mathbf{H}^{-1}\mathbf{C})$. Burnham & Anderson (2004) argue that the size of these matrices makes them difficult to estimate and that the TIC is likely close to the AIC when these matrices can be correctly estimated.

AIC, BIC, and TIC have seen little use in the context of deep networks. Rather, recent research has focused on developing new estimators. We briefly comment on the main approaches:

Flatness (Hochreiter & Schmidhuber, 1997) links the spectrum of the Hessian at a local optimum with the generalization gap. This correlation, observed again by Keskar et al. (2017), can be easily shown to not hold in general (Dinh et al., 2017), although it is possible that it does within the limited set of architectures and optimizers in use today. However, the use of flatness reveals a fundamental misunderstanding that we hope to clarify in this work.

Path-norm has been proposed by Neyshabur (2017) and uses special norms on the weights of the model to estimate the generalization gap. This work builds on the idea of *implicit regularization*, i.e., that our current optimizers implicitly follow a path leading to regularized solutions. While they show a good correlation with the true generalization gap in some situations, their measure is not fully robust to the transformations proposed by Dinh et al. (2017).

Sensitivity (Novak et al., 2018) links the generalization gap to the derivative of the loss with respect to the input. While this measure works well in the cases considered by the authors, it is not obvious to apply when the inputs are in a discrete set nor does it take the changes in the output into account.

Fisher-Rao norm (Liang et al., 2017) is equal to $\|\theta\|_{\mathbf{F}} = \sqrt{\theta^T \mathbf{F} \theta}$ where θ are the weights of the network. This work shows promising results, especially when \mathbf{C} is used instead of \mathbf{F} . Our work sheds light on why this is the case.

None of these measures incorporates knowledge about the uncertainty in data. For instance, it might happen that the derivative of the loss with respect to the input is very large in directions where there is no variation among training samples. In that case, it is reasonable to expect small variations in that direction in the test set and such directions should not impact the generalization gap. In this work, we argue that a meaningful measure should include knowledge about the variability in the data and not just about the curvature.

In some experiments of their paper, Liang et al. (2017) replace the Fisher matrix \mathbf{F} with the improperly named *empirical Fisher* matrix. This matrix is in fact the uncentered covariance matrix \mathbf{C} of the gradients. While it only differs from the Fisher matrix in the distribution under which the expectation is computed, the information encoded in this matrix is drastically different. The Fisher matrix is

a curvature matrix, encoding the local geometry of the model manifold (Amari, 1998), while the covariance matrix of the gradients encodes the uncertainty across datapoints. Section 3.1 clarifies the distinction between these quantities, which are known to be different (Le Roux et al., 2008; Martens, 2014; Liang et al., 2017) but are sometimes improperly used interchangeably.

3 Estimating the generalization gap using the Takeuchi information criterion

3.1 Setup and information matrices

Training a machine learning model is often cast as the minimization of a differentiable function \mathcal{L} over parameters θ in \mathbb{R}^d where d is the number of parameters in the model. To minimize this function, a standard assumption is that we have access to an oracle which, for every value of θ , returns both $\mathcal{L}(\theta)$ and the first derivative of \mathcal{L} with respect to θ , i.e., $\frac{\partial \mathcal{L}(\theta)}{\partial \theta}$. Given this oracle, first-order minimization methods iteratively perform the following update: $\theta_{t+1} = \theta_t - \alpha_t \frac{\partial \mathcal{L}(\theta_t)}{\partial \theta}$ where $\{\alpha_t\}_{t \geq 0}$ is a sequence of scalars called “stepsizes”.

Hessian. With some assumptions, this process converges to the unique minimizer θ^* of \mathcal{L} when the function is smooth and twice differentiable. The excess error $\mathcal{L}(\theta_t) - \mathcal{L}(\theta^*)$ decreases at a speed which depends on properties of its Hessian \mathbf{H} . Algorithms such as Gauss-Newton and L-BFGS (Nocedal & Wright, 2006) aim to use the curvature information contained in \mathbf{H} to transform \mathcal{L} in order to speed up optimization.

Fisher. First-order algorithms are sensitive to the particular parametrization chosen for \mathcal{L} . In cases where \mathcal{L} represents a negative conditional log-likelihood with $\mathcal{L}(\theta) = -\log q(\mathcal{D}|\theta)$ with \mathcal{D} a dataset of i.i.d samples, it is natural to perform first-order optimization in the natural space defined by the manifold of induced conditional distributions. Doing so requires access to another curvature matrix, \mathbf{F} , and leads to the natural gradient algorithm (Amari, 1998).

Covariance. In the context of machine learning where \mathcal{L} is often the average of a loss taken over N datapoints,² it might be computationally expensive to compute the gradient of the loss exactly. In these cases we replace the exact oracle with a noisy one and the update becomes $\theta_{t+1} = \theta_t - \alpha_t g_t$ where $g_t \in \mathbb{R}^d$ is a noisy estimate of the true gradient. In our setting, we will assume that our estimate is unbiased, i.e., $\mathbb{E}[g_t] = \frac{\partial \mathcal{L}(\theta_t)}{\partial \theta}$. The stochasticity of the oracle is another impediment of optimization and it is well-known that, in most cases, the excess error $\mathcal{L}(\theta_t) - \mathcal{L}(\theta^*)$ decreases far more slowly than in the noiseless case³. More precisely, the speed of convergence is also affected by the covariance matrix \mathbf{C} , defined as $\mathbf{C} = \mathbb{E}[g_t g_t^\top]$.

3.2 Specification and realizability

A parametric model q_θ is said to be *well specified* when there exists a parameter θ^* so that the true underlying data distribution is recovered, i.e $q_{\theta^*} = p$. We will make use of this concept several times in the following sections.

Realizability is a stronger notion, a model is *realizable* when there exists a parameter θ^* such that the true risk is 0; $\mathbb{E}_p[\mathcal{L}(\theta^*)] = 0$. This is for instance the case for a noiseless well-specified linear regression.

3.3 Generalization gap

When evaluating and training a model on the same data set, the training loss might not be a good estimator of the test performance. The discrepancy between these two losses is called the generalization gap \mathcal{G} .

²In the online case, we have $N = +\infty$.

³An exception to this is when the noise goes to 0 sufficiently fast as we approach the optimum.

While, in the machine learning community, cross-validation is the default choice for assessing the generalization of a model, other methods exist in the classical statistical literature. Commonly used are *information criteria* (IC), which attempt to build an estimator $\hat{\mathcal{G}}$ of the *generalization gap*.

3.3.1 Takeuchi information criterion for deep networks

In the simplest case of a well specified least squares regression problem, an unbiased estimator of the generalization gap is the AIC (Akaike, 1974), which is simply the number of degrees of freedom divided by the number of samples: $\hat{\mathcal{G}}(\theta) = \frac{1}{N}d$ where d is the dimensionality of θ . This estimator is valid locally around the maximum likelihood parameters computed on the training data.

However, these assumptions do not hold in most cases, leading to the number of parameters being a poor predictor of the generalization gap (Novak et al., 2018). When dealing with maximum likelihood estimation (MLE) in misspecified models, a more general formula for estimating the gap is given by the Takeuchi information criterion (TIC: Takeuchi, 1976):

$$\hat{\mathcal{G}} = \frac{1}{N} \text{Tr}(\mathbf{H}(\theta^*)^{-1} \mathbf{C}(\theta^*)) , \quad (1)$$

where θ^* is a local optimum. Note that \mathbf{H} and \mathbf{C} here are the hessian and covariance of the gradients matrices computed on the *true data distribution*. They can be estimated on test/validation data and evaluating them on train data gives a biased estimator we will refer to as "empirical TIC". This criterion is not new in the domain of machine learning. It was rediscovered by Murata et al. (1994) and similar criteria have been proposed since then (Beirami et al., 2017; Wang et al., 2018). However, as far as we know, no experimental validation of this criterion has been carried out for deep networks. Indeed, for deep networks, \mathbf{H} is highly degenerate, most of its eigenvalues being close to 0 (Sagun et al., 2016). In this work, the Takeuchi information criterion is computed, in the degenerate case, by only taking into account the eigenvalues of the Hessian of significant magnitude. In practice, we cut all the eigenvalues smaller than a constant times the biggest eigenvalue and perform the inversion on that subspace. Details can be found in appendix A.

3.3.2 The TIC and the generalization gap

We now empirically test the quality of the TIC as an estimator of the generalization gap in deep networks. Following Neyshabur et al. (2017) we assess the behaviour of our generalization gap estimator by varying (1) the number of parameters in a model and (2) the label randomization ratio.

Experiments are performed using a fully connected feedforward network with a single hidden layer trained on a subset of $2k$ samples of SVHN (Netzer et al., 2011). In Figure 1a we vary the number of units in the hidden layer without label randomization while in Figure 1b we vary the label randomization ratio with a fixed architecture. Each point is computed using 3 different random number generator seeds. The neural networks are trained for 750k steps. The confidence intervals are provided using bootstrapping to estimate a 95% confidence interval. The Hessian, covariance matrices and sensitivity are computed on a subset of size $5k$ of the test data. Details can be found in Appendix C.

We now study the ability of the TIC across a wide variety of models, datasets, and hyperparameters. More specifically, we compare the TIC to the generalization gap for:

- 5 different architectures: logistic regression, a 1-hidden layer and 2-hidden layer fully connected network, and 2 small convolutional neural networks (CNNs, one with batch normalization (Ioffe & Szegedy, 2015) and one without);
- 3 datasets: MNIST, CIFAR-10, SVHN;
- 3 learning rates: 10^{-2} , $5 \cdot 10^{-3}$, and 10^{-3} , using SGD with momentum $\mu = 0.9$;
- 2 batch sizes: 64, 512;
- 5 dataset sizes: 5k, 10k, 20k, 25k, and 50k.

We train for 750k steps and compute the metrics every 75k steps. To be able to compute the inverse of the Hessian without approximation, we chose neural networks architectures with a small number of parameters (a few thousands). To do so, we reduce the input dimension by converting all images to greyscale and resizing them to 7×7 pixels. While this makes the classification task more challenging,

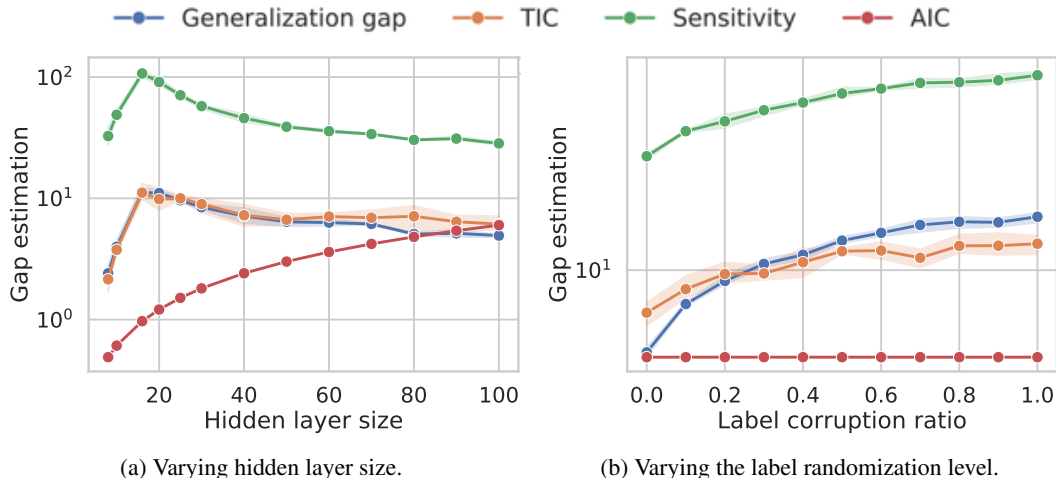


Figure 1: Comparing the TIC to other estimators of the generalization gap on SVHN. The TIC matches the generalization gap more closely than both the AIC and the sensitivity.

our neural networks still exhibit the behaviour of larger ones by their ability to fit the training set, even with random labels.

Figure 2a shows the results, with one plot per configuration, of the TIC when using the matrices \mathbf{H} and \mathbf{C} computed over the training set, which we denote by *empirical TIC*. While this experiment shows some correlation, it also shows that the empirical TIC underestimates the generalization gap. The outliers mainly correspond to networks trained MNIST or small subsets of CIFAR10 and SVHN. In these cases, the model is vastly overparametrized, thus the empirical covariance \mathbf{C} at a local optimum is often a poor estimate of the true covariance matrix of the gradients over the full distribution. Indeed, Figure 2b shows that the TIC using \mathbf{H} and \mathbf{C} computed over the test set is an excellent estimator of the generalization gap. For comparison, we also show in Figure 2d the generalization gap as a function of \mathbf{H} computed over the test set. We see that, even when using the test set, the correlation is much weaker than with the TIC.

4 Similarities and differences between information matrices

The previous section shed light on the performance of the TIC as an estimator of the generalization gap. From Eq. 1, we obtain that the TIC is equal to the number of parameters when $\mathbf{H} = \mathbf{C}$, a quantity known to be poorly correlated to the generalization gap. Hence, we conclude that these matrices are not equal in general. In this section, we explore the relationship between \mathbf{H} , \mathbf{F} and \mathbf{C} .

For this, we shall consider the case of maximum likelihood estimation (MLE). We will have access to a set of samples $(x, y) \in \mathcal{X} \times \mathcal{Y}$ where x is the input and y the target. We define $p : \mathcal{X} \times \mathcal{Y} \mapsto \mathbb{R}$ as the **data distribution** and $q_\theta : \mathcal{X} \times \mathcal{Y} \mapsto \mathbb{R}$ such that $q_\theta(x, y) = p(x)q_\theta(y|x)$ is the **model distribution**⁴. For each sample $(x, y) \sim p$, our loss is the negative log-likelihood $\ell_\theta(y, x) = -\log q_\theta(y|x)$.

Matrices \mathbf{H} , \mathbf{F} and \mathbf{C} are defined as:

⁴ $q_\theta(y|x)$ are the softmax activations of a neural network in the classification setting.

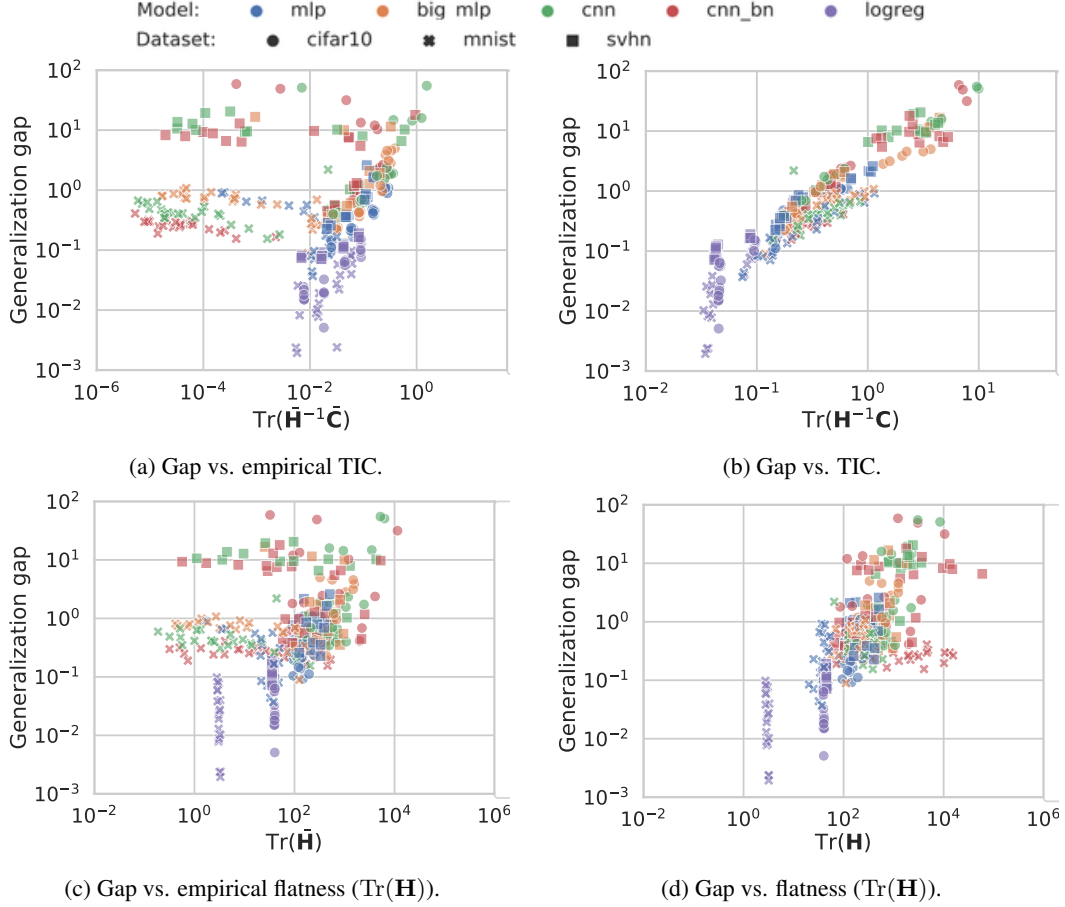


Figure 2: Generalization gap as a function of the empirical Takeuchi information criterion (*upper left*), the true TIC (*upper right*) and the trace of the Hessian on both the training (*bottom left*) and test set (*bottom right*) for many architectures, datasets, and hyperparameters. Correlation is perfect if all points lie on a line. We see that the Hessian cannot by itself capture the generalization gap.

$$\mathbf{H}(\theta) = \mathbb{E}_{x, y \sim p} \left[\frac{\partial^2}{\partial \theta \partial \theta^\top} \ell_\theta(y, x) \right] \quad (2)$$

$$\mathbf{C}(\theta) = \mathbb{E}_{x, y \sim p} \left[\frac{\partial}{\partial \theta} \ell_\theta(y, x) \frac{\partial}{\partial \theta} \ell_\theta(y, x)^\top \right] \quad (3)$$

$$\mathbf{F}(\theta) = \mathbb{E}_{x, y \sim q_\theta} \left[\frac{\partial}{\partial \theta} \ell_\theta(y, x) \frac{\partial}{\partial \theta} \ell_\theta(y, x)^\top \right] \quad (4)$$

$$= \mathbb{E}_{x, y \sim q_\theta} \left[\frac{\partial^2}{\partial \theta \partial \theta^\top} \ell_\theta(y, x) \right]. \quad (5)$$

We observe the following: a) The definition of \mathbf{H} and \mathbf{C} involves the data distribution, in contrast with the definition of \mathbf{F} , which involves the model distribution; b) If $q_\theta = p$, all matrices are equal. Furthermore, as noted by Martens (2014), $\mathbf{H} = \mathbf{F}$ whenever the matrix inside the expectation does not depend on y , a property shared in particular by all generalized linear models.

\mathbf{H} , \mathbf{F} , and \mathbf{C} characterize different properties of the optimization problem. \mathbf{H} and \mathbf{F} are curvature matrices and describe the geometry of the space around the current point. \mathbf{C} , on the other hand, is a “noise matrix” and represents the sensitivity of the gradient to the particular sample.⁵ As we observe

⁵Technically, it is Σ , the centered covariance matrix, rather than \mathbf{C} which plays that role but the two are similar close to a stationary point.

a lot of confusion about their similarities and differences, in past and current work, we clarify in the next subsections the role each of one has to play in machine learning.

4.1 Empirical Fisher does not approximate Fisher

\mathbf{C} is often referred to as the “empirical Fisher” matrix, implying that it is an approximation to the true Fisher matrix \mathbf{F} (Martens, 2014). In some recent works (Liang et al., 2017; George et al., 2018) the empirical Fisher matrix is used instead of the Fisher matrix. However, in the general case, there is no guarantee that \mathbf{C} will approximate \mathbf{F} , even in the limit of infinite samples. We now give a simple example highlighting their different roles.

Example 1 (Mean regression) Let $X = (x_i)_{i=1,\dots,N}$ be an i.i.d sequence of random variables. The task is to estimate $\mu = \mathbb{E}[x]$ by minimizing the loss $\mathcal{L}(\theta) = \frac{1}{2N} \sum_{n=1}^N \|x_n - \theta\|^2$. The minimum is attained at $\theta^{MLE} = \frac{1}{N} \sum_{n=1}^N x_n$. This estimator is consistent and converges to μ at rate $\mathcal{O}(\frac{1}{\sqrt{N}})$.

This problem is an MLE problem if we define $q_\theta(x) = \mathcal{N}(x; \theta, \mathbf{I}_d)$. In this case, we have

$$\mathbf{H}(\theta^{MLE}) = \mathbf{F}(\theta^{MLE}) = \mathbf{I}_d \quad , \quad \mathbf{C}(\theta^{MLE}) = \widehat{\Sigma}_x \quad , \quad (6)$$

where $\widehat{\Sigma}_x$ is the empirical covariance of the x_i 's. We see that, even in the limit of infinite data, the covariance \mathbf{C} does not converge to the actual Fisher matrix nor the Hessian. Hence we shall and will not refer to \mathbf{C} as the “empirical Fisher” matrix.

Concurrent to our work, Kunstner et al. (2019) highlighted limitations of the empirical Fisher approximation, both empirically and theoretically, and constructed examples where the empirical Fisher can be far from the true Fisher.

4.2 Well-specified models and information matrix equality

A model is *well-specified* when there exists θ^* such that $q_{\theta^*} = p$. For $\theta = \theta^*$, an identity between \mathbf{H} , \mathbf{C} and \mathbf{F} is verified

$$\mathbf{H}(\theta^*) = \mathbf{F}(\theta^*) = \mathbf{C}(\theta^*) \quad ,$$

which follows from eq. 2–4. This is called the *information matrix equality* (IME). In the above example, replacing the loss with $\mathcal{L}_{\Sigma_x}(\theta) = \frac{1}{2N} \sum_{n=1}^N (x_n - \theta)^\top \Sigma_x^{-1} (x_n - \theta)$, the log-likelihood of the well-specified model, leads to the IME.

Hence, even though the optimum of the two problems is the same and the same predictions on the test set will be made, this change can make or break the equivalence between information matrices. Note that when the IME holds, the TIC can be simplified as $\frac{1}{N} \text{Tr}(\mathbf{I}_d) = \frac{1}{N} d$ thus recovering the AIC. To conclude, these three matrices are only equal at the optimum of a well-specified model and not in the general case.

4.3 The importance of the noise in estimating the generalization gap

For a given model, the generalization gap captures the discrepancy that exists between the training set and the data distribution. Hence, estimating that gap involves the evaluation of the uncertainty around the data distribution. The TIC uses \mathbf{C} to capture that uncertainty but other measures probably exist. However, estimators which do not estimate it are bound to have failure modes. For instance, by using the square norm of the derivative of the loss with respect to the input, the sensitivity implicitly assumes that the uncertainty around the inputs is isotropic and will fail should the data be heavily concentrated in a low-dimensional subspace. It would be interesting to adapt the sensitivity to take the covariance of the inputs into account.

Another aspect worth mentioning is that estimators such as the margin assume that the classifier is fixed but the data is a random variable. Then, the margin quantifies the probability that a new datapoint would fall on the other side of the decision boundary. By contrast, the TIC assumes that the data are fixed but that the classifier is a random variable. It estimates the probability that a classifier

trained on slightly different data would classify a training point incorrectly. In that, it echoes the uniform stability theory (Bousquet & Elisseeff, 2002), where a full training with a slightly different training set has been replaced with a local search.

4.4 Experiments and TIC proxies

4.4.1 Discrepancies between \mathbf{C} , \mathbf{H} and \mathbf{F}

In this subsection, we analyze the similarities and differences between the information matrices. We will focus on the scale similarity r , defined as the ratio of traces, and the angle similarity s , defined as the cosine between matrices. Note that $r(\mathbf{A}, \mathbf{B}) = 1$ and $s(\mathbf{A}, \mathbf{B}) = 1$ implies $\mathbf{A} = \mathbf{B}$.

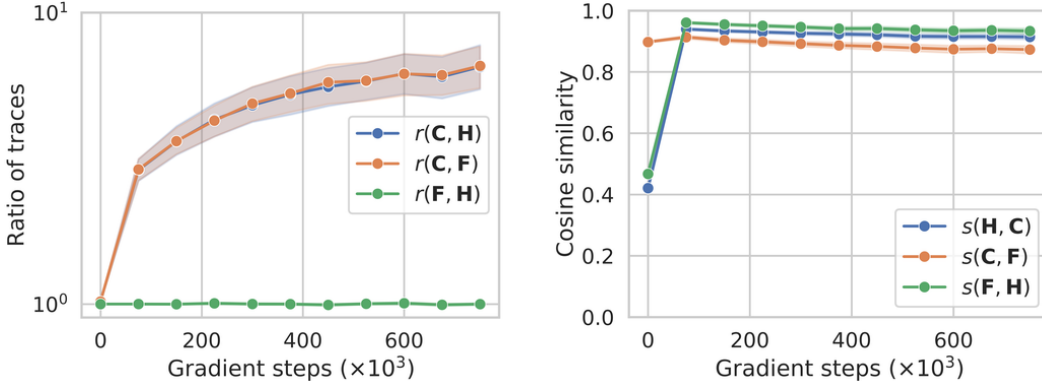


Figure 3: Scale and angle similarities between information matrices.

Figure 3 shows the scale (left) and angle (right) similarities between the three pairs of matrices during the optimization of all models used in figure 2. We can see that \mathbf{H} is not aligned with \mathbf{C} nor \mathbf{F} at the beginning of the optimization but this changes quickly. Then, all three matrices reach a very high cosine similarity. For the scaling, \mathbf{C} is “larger” than the other two while \mathbf{F} and \mathbf{H} are very close to each other.

4.4.2 Fisher vs “empirical Fisher”

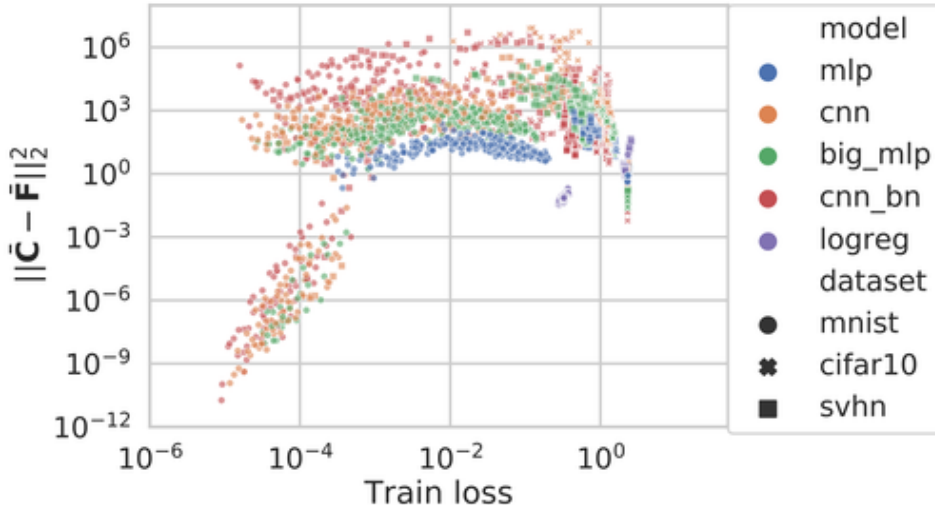


Figure 4: Squared Frobenius norm between $\bar{\mathbf{F}}$ and $\bar{\mathbf{C}}$ (computed on the training distribution). Even for some low training losses, there can be a significant difference between the two matrices.

Although we have shown in the previous subsection that \mathbf{F} can potentially be arbitrarily far from \mathbf{C} , this does not imply that they cannot be close in practice, if only because, for vastly overparametrized

models, one would hope that $q_\theta(y|x)$ matches $p(y|x)$. Figure 4 shows the squared Frobenius norm between \mathbf{F} and \mathbf{C} for many architectures, datasets, at various stages of the optimization. We see that, while the two matrices eventually coincide on the training set, the convergence is very weak as even low training errors can lead to a large discrepancy between these two matrices. This confirms some observations made by Kunstner et al. (2019), in practice, \mathbf{C} and \mathbf{F} might be significantly different, even when computed on the training set. We do also provide theoretical bounds for the L_2 distance between all the information matrices in appendix F.

4.4.3 Efficient approximations to the TIC

Although the TIC is a good estimate of the generalization gap, it can be expensive to compute on large models. Following our theoretical and empirical analysis of the proximity of \mathbf{H} and \mathbf{F} , we propose two approximations to the TIC: $\text{Tr}(\mathbf{F}^{-1}\mathbf{C})$ and $\text{Tr}(\mathbf{C})/\text{Tr}(\mathbf{F})$. They are easier to compute as the \mathbf{F} is in general easier to compute than \mathbf{H} and the second does not require any matrix inversion.

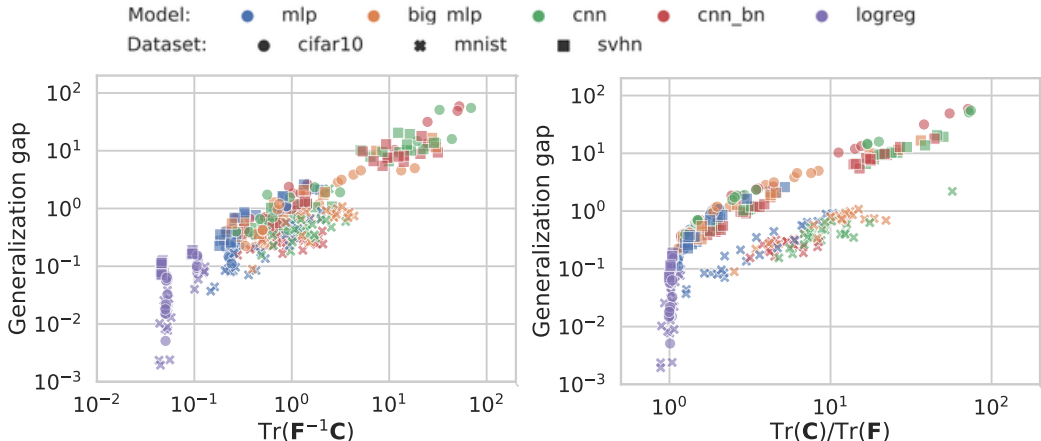


Figure 5: Generalization gap as a function of two approximations to the Takeuchi Information Criterion: $\text{Tr}(\mathbf{F}^{-1}\mathbf{C})$ (left) and $\text{Tr}(\mathbf{C})/\text{Tr}(\mathbf{F})$ (right).

Using the same experimental setting as in 3.3.2, we observe in Figure 5 that the replacing \mathbf{H} with \mathbf{F} leads to almost no loss in predictive performance. On the other hand, the ratio of the traces works best when the generalization gap is high and tends to overestimate it when it is small.

Intuition on $\text{Tr}(\mathbf{C})/\text{Tr}(\mathbf{F})$: it is not clear right away why the ratio of traces might be an interesting quantity. However, as observed in figure 3, \mathbf{C} and \mathbf{F} are remarkably aligned, but there remains a scaling factor. If we had $\mathbf{C} = \alpha\mathbf{F}$, then $\text{Tr}(\mathbf{F}^{-1}\mathbf{C}) = k\alpha$ where k is the dimension of the invertible subspace of \mathbf{F} and $\text{Tr}(\mathbf{C})/\text{Tr}(\mathbf{F}) = d\alpha$ where d is the dimensionality of θ . So, up to a multiplicative constant (or an offset in log scale), we can expect these two quantities to exhibit similarities. Notice that on figure 5, this offset does appear and is different for every dataset (MNIST has the smallest one, then SVHN and CIFAR10, just slightly bigger).

5 Open questions

5.1 Dynamics of SGD

Zhang et al. (2016) conjectured that stochastic gradient descent (SGD) might perform an implicit regularization for deep learning models as it does for linear ones. Several recent works have studied the dynamics of SGD as a continuous time stochastic differential equation (SDE) (Mandt et al., 2017; Jastrzyski et al., 2017; Chaudhari & Soatto, 2017). In the simple case where we assume being in the neighborhood of an optimum θ^* and that \mathbf{H} and \mathbf{C} are locally constant, then the continuous time SDE that governs SGD is an Ornstein-Uhlenbeck process (Heskes & Kappen, 1993; Mandt et al., 2017; Antognini & Sohl-Dickstein, 2018). For such process, the stationary distribution of θ can be computed in closed form, it is a Gaussian $\mathcal{N}(\theta; \theta^*, \Sigma^*)$, where Σ^* is solution of the Lyapunov

equation $\mathbf{H}\Sigma^* + \Sigma^*\mathbf{H} = \frac{\eta}{m}\mathbf{C}$ with η the learning rate and m the minibatch size. See appendix E for details.

Notably, provided \mathbf{H} is invertible, we have that: $\text{Tr}(\Sigma^*) = \frac{\eta}{2m} \text{Tr}(\mathbf{H}^{-1}\mathbf{C})$.

This highlights a connection between the limit cycles of SGD and the TIC (on the training set). We believe SGD might be prone to seek regions of the parameter space with a low variance. Intuitively, for two minima with the same depth, the SGD process might be more stable in the minimum with lower variance, i.e., in the minimum where the empirical TIC is lower, hence potentially in regions of the parameter space where the generalization gap is lower.

5.2 \mathbf{H} vs. \mathbf{C} as acceleration vs. noise reduction

Several well-known algorithms, such as Adam (Kingma & Ba, 2014), claiming to use second-order information about the loss to accelerate training seem instead to be using the covariance matrix of the gradients. Equipped with this new understanding of the difference between the curvature and noise information matrices, one might wonder if the success of these methods is not due to variance reduction instead. If so, one should be able to combine variance reduction and geometry adaptation, an idea attempted by Le Roux et al. (2011).

6 Conclusion

We have investigated whether the Takeuchi information criterion is relevant for estimating the generalization gap in neural networks. We have provided evidence that this complexity measures involving the information matrices is predictive of the generalization performance. We then studied the similarities and discrepancies between these matrices, shedding light on some common misconceptions. This theoretical and empirical analyses yielded insights on the similarity between the Fisher matrix and the Hessian. We then used these results to propose two measures approximating the TIC, but far more efficient to compute.

Finally we drew links between the TIC and the limit cycles of SGD, conjecturing that SGD might implicitly bias the optimization towards regions of low complexity. We furthermore pointed out that many algorithms trying to do second order optimization might actually be performing variance reduction.

We hope this study will clarify the interplay of the noise and curvature in common machine learning settings, potentially giving rise to new algorithms.

Acknowledgments

We would like to thank Gauthier Gidel, Reyhane Askari and Giancarlo Kerg for reviewing an earlier version of this paper. We also thank Aristide Baratin for insightful discussions. Valentin Thomas acknowledges funding from the Open Philanthropy project.

References

- Akaike, Hirotugu. A new look at the statistical model identification. *IEEE transactions on automatic control*, 19(6):716–723, 1974.
- Amari, Shun-Ichi. Natural gradient works efficiently in learning. *Neural computation*, 10(2):251–276, 1998.
- Antognini, Joseph M and Sohl-Dickstein, Jascha. PCA of high dimensional random walks with comparison to neural network training. *arXiv preprint arXiv:1806.08805*, 2018.
- Beirami, Ahmad, Razaviyayn, Meisam, Shahrampour, Shahin, and Tarokh, Vahid. On optimal generalizability in parametric learning. In *Advances in Neural Information Processing Systems*, pp. 3455–3465, 2017.
- Boué, Laurent. Real numbers, data science and chaos: How to fit any dataset with a single parameter. *arXiv preprint arXiv:1904.12320*, 2019.

- Bousquet, Olivier and Elisseeff, André. Stability and generalization. *Journal of machine learning research*, 2(Mar):499–526, 2002.
- Burnham, Kenneth P and Anderson, David R. Multimodel inference: understanding aic and bic in model selection. *Sociological methods & research*, 33(2):261–304, 2004.
- Chaudhari, Pratik and Soatto, Stefano. Stochastic gradient descent performs variational inference, converges to limit cycles for deep networks. *arXiv preprint arXiv:1710.11029*, 2017.
- Dinh, Laurent, Pascanu, Razvan, Bengio, Samy, and Bengio, Yoshua. Sharp minima can generalize for deep nets. *International Conference on Machine Learning (ICML)*, 2017.
- Efron, Bradley. Bootstrap methods: another look at the jackknife. In *Breakthroughs in statistics*, pp. 569–593. Springer, 1992.
- George, Thomas, Laurent, César, Bouthillier, Xavier, Ballas, Nicolas, and Vincent, Pascal. Fast approximate natural gradient descent in a kronecker factored eigenbasis. In *Advances in Neural Information Processing Systems*, pp. 9550–9560, 2018.
- Hastie, Trevor, Tibshirani, Robert, and Friedman, Jerome. *The elements of statistical learning: data mining, inference, and prediction*. New York, NY: Springer, 2009.
- Heskes, Tom M and Kappen, Bert. On-line learning processes in artificial neural networks. In *North-Holland Mathematical Library*, volume 51, pp. 199–233. Elsevier, 1993.
- Hochreiter, Sepp and Schmidhuber, Jürgen. Flat minima. *Neural Computation*, 9(1):1–42, 1997.
- Ioffe, Sergey and Szegedy, Christian. Batch normalization: Accelerating deep network training by reducing internal covariate shift. *arXiv preprint arXiv:1502.03167*, 2015.
- Jastrzębski, Stanisław, Kenton, Zachary, Arpit, Devansh, Ballas, Nicolas, Fischer, Asja, Bengio, Yoshua, and Storkey, Amos. Three factors influencing minima in sgd. *arXiv preprint arXiv:1711.04623*, 2017.
- Keskar, Nitish Shirish, Mudigere, Dheevatsa, Nocedal, Jorge, Smelyanskiy, Mikhail, and Tang, Ping Tak Peter. On large-batch training for deep learning: Generalization gap and sharp minima. *International Conference on Learning Representations (ICLR)*, 2017.
- Kingma, Diederik P and Ba, Jimmy. Adam: A method for stochastic optimization. *arXiv preprint arXiv:1412.6980*, 2014.
- Kunstner, Frederik, Balles, Lukas, and Hennig, Philipp. Limitations of the empirical fisher approximation. *arXiv preprint arXiv:1905.12558*, 2019.
- Le Roux, Nicolas, Manzagol, Pierre-Antoine, and Bengio, Yoshua. Topmoumoute online natural gradient algorithm. In *Advances in neural information processing systems*, pp. 849–856, 2008.
- Le Roux, Nicolas, Bengio, Yoshua, and Fitzgibbon, Andrew. Improving first and second-order methods by modeling uncertainty. *Optimization for Machine Learning*, pp. 403, 2011.
- Liang, Tengyuan, Poggio, Tomaso, Rakhlin, Alexander, and Stokes, James. Fisher-rao metric, geometry, and complexity of neural networks. *arXiv preprint arXiv:1711.01530*, 2017.
- Mandt, Stephan, Hoffman, Matthew D, and Blei, David M. Stochastic gradient descent as approximate bayesian inference. *The Journal of Machine Learning Research*, 18(1):4873–4907, 2017.
- Martens, James. New insights and perspectives on the natural gradient method. *arXiv preprint arXiv:1412.1193*, 2014.
- Murata, Noboru, Yoshizawa, Shuji, and Amari, Shun-ichi. Network information criterion-determining the number of hidden units for an artificial neural network model. *IEEE Transactions on Neural Networks*, 5(6):865–872, 1994.
- Netzer, Yuval, Wang, Tao, Coates, Adam, Bissacco, Alessandro, Wu, Bo, and Ng, Andrew Y. Reading digits in natural images with unsupervised feature learning. *Neural Information Processing Systems (NeurIPS)*, 2011.

- Neyshabur, Behnam. Implicit regularization in deep learning. *arXiv preprint arXiv:1709.01953*, 2017.
- Neyshabur, Behnam, Bhojanapalli, Srinadh, McAllester, David, and Srebro, Nati. Exploring generalization in deep learning. In *Advances in Neural Information Processing Systems*, pp. 5947–5956, 2017.
- Nocedal, Jorge and Wright, Stephen. *Numerical optimization*. Springer Science & Business Media, 2006.
- Novak, Roman, Bahri, Yasaman, Abolafia, Daniel A, Pennington, Jeffrey, and Sohl-Dickstein, Jascha. Sensitivity and generalization in neural networks: an empirical study. *International Conference on Learning Representations (ICLR)*, 2018.
- Rangamani, Akshay, Nguyen, Nam H, Kumar, Abhishek, Phan, Dzung, Chin, Sang H, and Tran, Trac D. A scale invariant flatness measure for deep network minima. *arXiv preprint arXiv:1902.02434*, 2019.
- Sagun, Levent, Bottou, Léon, and LeCun, Yann. Eigenvalues of the hessian in deep learning: Singularity and beyond. *arXiv preprint arXiv:1611.07476*, 2016.
- Schwarz, Gideon et al. Estimating the dimension of a model. *The annals of statistics*, 6(2):461–464, 1978.
- Stone, Mervyn. Cross-validators choice and assessment of statistical predictions. *Journal of the Royal Statistical Society: Series B (Methodological)*, 36(2):111–133, 1974.
- Takeuchi, Kei. The distribution of information statistics and the criterion of goodness of fit of models. *Mathematical Science*, 153:12–18, 1976.
- Wang, Shuaiwen, Zhou, Wenda, Lu, Haihao, Maleki, Arian, and Mirrokni, Vahab. Approximate leave-one-out for fast parameter tuning in high dimensions. *arXiv preprint arXiv:1807.02694*, 2018.
- Zhang, Chiyuan, Bengio, Samy, Hardt, Moritz, Recht, Benjamin, and Vinyals, Oriol. Understanding deep learning requires rethinking generalization. *arXiv preprint arXiv:1611.03530*, 2016.

A Details on the Hessian inverse

As \mathbf{H} is highly degenerate in neural networks, we compute an inverse of \mathbf{H} by cutting all the eigenvalues smaller than $10^{-3} \times \lambda_{max}$ where λ_{max} is the biggest eigenvalue of \mathbf{H} . We observed that 10^{-3} and 10^{-3} were reasonable constants for selecting the eigenvalues of significant magnitude. Using smaller constant sometimes lead to very noisy estimates of the TIC while using a bigger constant would lead to severe underestimation of the criterion.

B Details on the Information Matrix Equality

To understand the IME, one needs to show the equivalence between the two definitions of \mathbf{F} eq 4 and eq 5.

A concise proof can be found on the Wikipedia page of the Fisher Information Matrix https://en.wikipedia.org/wiki/Fisher_information.

C Details on the large scale experiments

These details apply for the experiments conducted in subsection 3.3.2, figure 2 and all figures in subsection 4.4.

We remind the reader the setup.

- 5 different architectures: logistic regression, a 1-hidden layer and 2-hidden layer fully connected network, and 2 small convolutional neural networks (CNNs, one with batch normalization (Ioffe & Szegedy, 2015) and one without);
- 3 datasets: MNIST, CIFAR-10, SVHN;
- 3 learning rates: 10^{-2} , $5 \cdot 10^{-3}$, 10^{-3} using vanilla SGD with momentum $\mu = 0.9$;
- 2 batch sizes: 64, 512;
- 5 dataset sizes: 5k, 10k, 20k, 25k, 50k.

We train for 750k steps and compute our metrics every 75k steps.

Data preprocessing: We choose to greyscale, resize to 7×7 pixels and normalize all the images in the 3 datasets used (CIFAR-10, MNIST and SVHN). This way, we can design architectures with a relatively low number of parameters.

Architectures:

- `mlp`: This one is a one hidden layer MLP. Input size is $7 \times 7 = 49$ and output size is 10. The default number of hidden units is 70. We use ReLU activations.
- `big_mlp`: The architecture is the same as above but with one additional hidden layer.
- `logreg`: This is simple a 49×10 linear classifier.
- `cnn`: It is a small CNN with 3 layers. A first conv layer with kernel 3×3 , 0 padding and 15 channels. The next layer has 20 channels and same parameters. The last layer has 10 channels and directly outputs the class scores.
- `cnn_bn`: Same architecture as above, except for a spatial batch-norm after the second layer.

D Details on experiments of subsection 3.3.2

For these experiments we train one hidden layer MLPs on SVHN. Each points is computed by training three times with three different random seed until convergence. In figure 1a, the labels are kept without corruption and we vary the hidden size layer by using $\{8, 10, 16, 20, 25, 30, 40, 50, 60, 70, 80, 100\}$ hidden units in the hidden layer.

In figure 1b, we fix the number of hidden units to 70 but we vary the labels corruption percentage from 0% to 100% (included) by increments of 10%.

The networks are trained for 150k gradients steps with a learning rate of $5 \cdot 10^{-3}$ and a batch size of 256. We used a subset of 2000 samples of SVHN to remain in the highly overparametrized regime, our networks were able to fit random data.

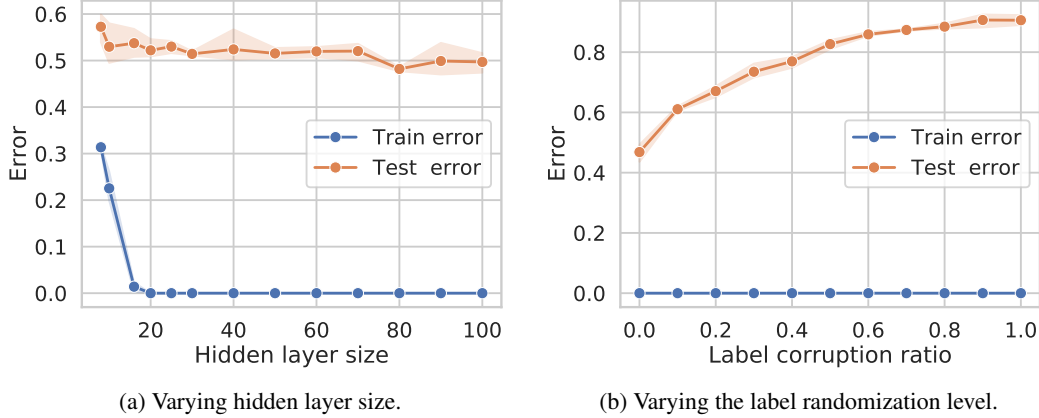


Figure 6: The train and test errors associated with the experiments 1a and 1b. We see that while we use small networks, they are still able to fit the data completely provided we use more than 20 hidden units. This behavior mirrors the one of bigger networks.

E TIC and dynamics of SGD

E.1 SGD as a continuous time SDE

The continuous-time stochastic differential equation that governs SGD can be written:

$$d\theta_t = -\eta \nabla_{\theta} \mathcal{L}(\theta) dt + \frac{\eta}{\sqrt{m}} \mathbf{C}^{\frac{1}{2}} dW_t,$$

with η the learning rate, m the minibatch size, $\mathbf{C}^{\frac{1}{2}} \mathbf{C}^{\frac{1}{2}\top} = \mathbf{C}$ the centered gradients' covariance and W_t is a Wiener process. There are implicit assumption to obtain this equation, namely that discretet-time SGD can be indeed approximated as a continuous process and that for m sufficiently large, the Central Limit Theorem applies and thus the noise on the gradient is approximately Gaussian, hence the Wiener process.

When we assume being in the neighborhood of an optimum θ^* and that \mathbf{H} and \mathbf{C} are locally constant, the equation above can be approximated by an Ornstein-Uhlenbeck process (Heskes & Kappen, 1993; Mandt et al., 2017; Antognini & Sohl-Dickstein, 2018):

$$d\theta_t = -\eta \mathbf{H}(\theta_t - \theta^*) dt + \frac{\eta}{\sqrt{m}} \mathbf{C}^{\frac{1}{2}} dW_t.$$

E.2 Limit cycles of SGD

By doing the change of variable $\phi_t = e^{-\eta \mathbf{H} t} \theta_t$ We have $d\phi_t = e^{-\eta \mathbf{H} t} (-\eta \mathbf{H} \theta_t dt + d\theta_t) = e^{-\eta \mathbf{H} t} \frac{\eta}{\sqrt{m}} \mathbf{C}^{\frac{1}{2}} dW_t$. Therefore

$$\theta_t = \frac{\eta}{\sqrt{m}} e^{\eta \mathbf{H} t} \int_0^t e^{-\eta \mathbf{H} s} \mathbf{C}^{\frac{1}{2}} dW_s + \theta^* + e^{-\eta \mathbf{H} t} (\theta_0 - \theta^*).$$

Hence

$$\Sigma_t = \text{Cov}[\theta_t] = \frac{\eta^2}{m} \int_0^t e^{-\eta \mathbf{H} s} \mathbf{C} e^{-\eta \mathbf{H} s} ds$$

using Ito isometry.

This matrix is positive and $\Sigma_\infty = \lim_{t \rightarrow \infty} \Sigma_t$ verifies the Lyapunov equation (Mandt et al., 2017): $\mathbf{H}\Sigma_\infty + \Sigma_\infty\mathbf{H} = \frac{\eta}{m}\mathbf{C}$.

Notably, if \mathbf{H} is invertible, we have that:

$$\text{Tr}(\Sigma_\infty) = \frac{\eta}{2m} \text{Tr}(\mathbf{H}^{-1}\mathbf{C})$$

F Bounds between \mathbf{H} , \mathbf{F} and \mathbf{C}

$$\begin{aligned} |\mathbf{F}_{ij} - \mathbf{H}_{ij}|^2 &= \left| \int q_\theta(x, y) (\nabla_\theta^2 \mathcal{L}(x, y))_{ij} d(x, y) - \int p(x, y) (\nabla_\theta^2 \mathcal{L}(x, y))_{ij} d(x, y) \right|^2 \\ &= \left| \int (q_\theta(x, y) - p(x, y)) (\nabla_\theta^2 \mathcal{L}(x, y))_{ij} d(x, y) \right|^2 \\ &= \left| \int \frac{(q_\theta(x, y) - p(x, y))}{\sqrt{p(x, y)}} (\sqrt{p(x, y)} \nabla_\theta^2 \mathcal{L}(x, y))_{ij} d(x, y) \right|^2 \\ &\leq \int \frac{(q_\theta(x, y) - p(x, y))^2}{p(x, y)} d(x, y) \int p(x, y) (\nabla_\theta^2 \mathcal{L}(x, y))_{ij}^2 d(x, y) \\ &= \mathcal{D}_{\chi^2}(p||q_\theta) \mathbb{E}_p[(\nabla_\theta^2 \mathcal{L}(x, y))_{ij}^2] \end{aligned}$$

Where we used Cauchy-Schwarz inequality and gD_{χ^2} denotes the χ^2 divergence.

$$\|\mathbf{F} - \mathbf{H}\|^2 \leq \mathcal{D}_{\chi^2}(p||q_\theta) \mathbb{E}_p[\|\mathbf{H}(x, y)\|_2^2]$$

Where $\mathbf{H}(x, y) \triangleq \nabla_\theta^2 \mathcal{L}(x, y)$ is the empirical hessian for one sample and the $\|\cdot\|_2$ is the Frobenius norm.

In the same way

$$\begin{aligned} |\mathbf{F}_{ij} - \mathbf{C}_{ij}|^2 &= \left| \int q_\theta(x, y) (\nabla_\theta \mathcal{L}(x, y) \nabla_\theta \mathcal{L}(x, y)^\top)_{ij} d(x, y) - \int p(x, y) (\nabla_\theta \mathcal{L}(x, y) \nabla_\theta \mathcal{L}(x, y)^\top)_{ij} d(x, y) \right|^2 \\ &\leq \mathcal{D}_{\chi^2}(p||q_\theta) \mathbb{E}_p[(\nabla_\theta \mathcal{L}(x, y) \nabla_\theta \mathcal{L}(x, y)^\top)_{ij}^2] \end{aligned}$$

For $\mathbf{C}(x, y) \triangleq \nabla_\theta \mathcal{L}(x, y) \nabla_\theta \mathcal{L}(x, y)^\top$ we have

$$\|\mathbf{F} - \mathbf{C}\|^2 \leq \mathcal{D}_{\chi^2}(p||q_\theta) \mathbb{E}_p[\|\mathbf{C}(x, y)\|^2]$$

Hence

$$\|\mathbf{C} - \mathbf{H}\|^2 \leq \mathcal{D}_{\chi^2}(p||q_\theta) \mathbb{E}_p[\|\mathbf{C}(x, y)\|^2 + \|\mathbf{H}(x, y)\|^2]$$